Effects of 2.6-GeV U ion irradiation on the superconductivity of the kagome superconductors CsV_3Sb_5 and $Cs(V_{0.93}Nb_{0.07})_3Sb_5$

Chunlei Wang,[1,2] Lubin Wang,[2] Yuki Hirota,[1] Wenjie Li,[1] Ryosuke Sakagami,[1] Yongkai Li,[3,4] Ataru Ichinose,[5] Xiaolei Yi,[2] Yangsong Chen,[1] Cheng Yu,[1] Zhiwei Wang,[3,4,*] and Tsuyoshi Tamegai[1,†]

[1]*Department of Applied Physics, The University of Tokyo, Tokyo 113-8656, Japan*

[2]*Department of Physics and Electronic Engineering, Xinyang Normal University, Xinyang 464000, China*

[3]*Centre for Quantum Physics, Key Laboratory of Advanced Optoelectronic Quantum Architecture and Measurement (MOE), School of Physics, and Beijing Key Lab of Nanophotonics and Ultrafine Optoelectronic Systems, Beijing Institute of Technology, Beijing 100081, China*

[4]*Material Science Center, Yangtze Delta Region Academy of Beijing Institute of Technology, Jiaxing 314011, China*

[5]*Central Research Institute of Electric Power Industry, Electric Power Engineering Research Laboratory, Nagasaka, Yokosuka-shi, Kanagawa, 240-0196, Japan*

(Received 14 April 2024; revised 4 July 2024; accepted 5 August 2024; published 26 August 2024)

We have investigated the effect of 2.6-GeV U irradiation on the superconductivity of CsV_3Sb_5 and $Cs(V_{0.93}Nb_{0.07})_3Sb_5$ single crystals by using resistivity and magnetization measurements. The critical transition temperature for CsV_3Sb_5 crystal is enhanced up to 4.3 K after irradiation with a dose of $B_\Phi = 2.0$ T, while the critical current density is increased up to $\sim 0.8 \times 10^4$ A/cm^2 after irradiation with a dose of $B_\Phi = 0.5$ T under self-field at 2.0 K, which is about four times larger than that for the pristine crystal under the same condition. For $Cs(V_{0.93}Nb_{0.07})_3Sb_5$ crystal, the critical transition temperature remains almost constant up to $B_\Phi = 2.0$ T, followed by monotonic suppression with further increase of dose. Besides the enhanced critical current density, we observe an anomalous peak effect in the magnetic hysteresis loop close to zero field at low irradiation doses, which can be interpreted by the matching effect in irradiated $Cs(V_{0.93}Nb_{0.07})_3Sb_5$ crystals.

DOI: 10.1103/PhysRevB.110.054520

I. INTRODUCTION

Kagome materials are currently a hot topic in the field of condensed matter physics [1–3]. The electronic structure of kagome materials usually demonstrates interesting features such as a flat energy band, van Hove singularity, and Dirac or Weyl point. Thus, a wide variety of quantum states are expected, including bond-density wave order, charge-density waves (CDWs), spin-density waves (SDWs), and spin liquid states, in addition to superconductivity by adjusting the band filling [4–9]. Recently, a new family of kagome compounds, AV_3Sb_5 (A = K, Rb, or Cs), was reported containing the 3d transition metal vanadium [10]. Subsequently, superconductivity, CDWs with time-reversal symmetry breaking, in-plane nematic order, and the giant anomalous Hall effect have been observed in the system [11–17]. The coexistence and competition between superconductivity and CDWs make these materials much more interesting. For example, two superconducting domes and a completely suppressed CDW transition have been observed in hole-doped samples, such as $CsV_{3-x}Ti_xSb_5$ and $CsV_3Sb_{5-x}Sn_x$ [18–20], while the enhanced superconductivity and suppressed CDW have been found in samples with isoelectronic dopings [21–23]. Besides the chemical doping, high pressure is another effective method to adjust the quantum state in the system. It has been reported that superconductivity shows two-dome-like behavior under moderate pressure and the CDW is monotonically suppressed by pressure [24–26].

High-energy ion irradiation is one of the effective methods to control superconductivity, especially for superconductors with competing orders. For example, the critical transition temperature, T_c, can be enhanced up to 7.5 K in $NbSe_2$ after electron irradiation [27]. Roppongi *et al.* found that both T_c and the CDW of CsV_3Sb_5 are suppressed after 2.5-MeV electron irradiation [28]. Recently, we found that 3-MeV proton irradiation enhances T_c concomitant with suppression of the CDW in CsV_3Sb_5 [29]. In contrast to light-particle irradiations, heavy-ion irradiations have been considered to be much more effective at modifying vortex dynamics due to the larger damaged volume fraction at the same dose [30]. Additionally, due to the geometrical similarity between vortices and defects, the columnar defects produced by heavy-ion irradiation usually give better pinning properties than point defects introduced by light-particle irradiations [30,31]. In the present study, we have conducted 2.6-GeV U irradiation experiments into CsV_3Sb_5 and $Cs(V_{0.93}Nb_{0.07})_3Sb_5$ single crystals. A systematic investigation on the effect of heavy-ion irradiation on superconductivity in these kagome superconductors is reported.

II. EXPERIMENTAL METHODS

Single crystals of CsV_3Sb_5 and $Cs(V_{0.93}Nb_{0.07})_3Sb_5$ were grown by the self-flux method, with the Cs-Sb binary

*Contact author: zhiweiwang@bit.edu.cn
†Contact author: tamegai@ap.t.u-tokyo.ac.jp

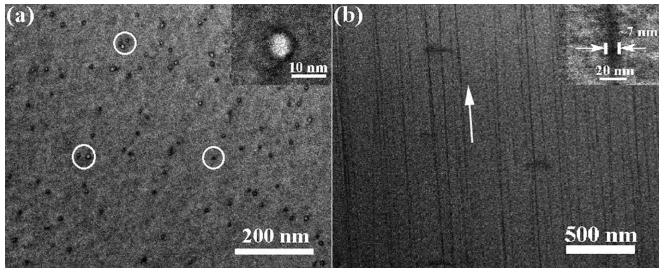

FIG. 1. STEM images of $Cs(V_{0.93}Nb_{0.07})_3Sb_5$ irradiated by 2.6-GeV U at $B_\Phi = 1$ T. (a) Plan view: complete circles indicate locations of columnar defects. (b) Cross section: the arrow indicates the c axis. The insets of (a) and (b) show magnifications of each image, indicating an average diameter of the columnar defect is ~7 nm.

eutectic mixture $Cs_{0.4}Sb_{0.6}$ as the flux. The mixture was put into an alumina crucible and then the crucible was sealed in a quartz tube [22]. The 2.6-GeV U irradiation was performed using a ring cyclotron at the RI Beam Factory operated by RIKEN Nishina Center and CNS. The projected range of the 2.6-GeV U ion in the CsV_3Sb_5 system is ~71 μm, which was calculated by the SRIM program [32]. In the present experiment, all the samples were cleaved into thin flakes with thickness less than ~40 μm. All irradiations were carried out at room temperature in vacuum better than 1×10^{-5} Torr. The irradiation dose is labeled by the matching field, B_Φ, which is related to the density of columnar defects, n (cm^{-2}), as $B_\Phi = n\Phi_0$, where $\Phi_0 (= 2.07 \times 10^{-11}$ T $cm^2)$ is the flux quantum. Namely, $B_\Phi = 1$ T corresponds to $n = 5 \times 10^{10}$ cm^{-2}. The crystal structure was determined at room temperature by using a commercial diffractometer (Smartlab, Rigaku) with Cu $K\alpha$ radiation. The measurements of resistivity and magnetization were carried out using DynaCool-PPMS-9T (Quantum Design) and a superconducting quantum interference device (SQUID) magnetometer (MPMS-XL5, Quantum Design). Critical current density (J_c) is evaluated magnetically using the extended Bean model.

III. RESULTS AND DISCUSSION

Figure 1(a) shows a scanning transmission electron microscopy (STEM) image of defects in $Cs(V_{0.93}Nb_{0.07})_3Sb_5$ irradiated by 2.6-GeV U at $B_\Phi = 1$ T along the incident ion beam (plan view). The columnar defects, some of which are marked by circles, appear as circular dots indicating almost isotropic structural damage in the ab plane as shown in the inset of Fig. 1(a). Small differences in sharpness at the edge indicate that some of the ion projectiles were weakly scattered after they entered the crystal. Figure 1(b) shows a cross-section view, which is elongated and looks like rods. It is clear that the defects are ion trajectories or ion tracks. The contrast between the ion tracks and matrix reflects the presence of strain in the area of structural damage. Similar to those in 2.6-GeV U-irradiated K-doped $BaFe_2As_2$ [33], these defects are continuous. These defects have similar structure with vortices, which can serve as effective pinning centers and enhance the critical current density greatly. The average density of defects is about 3.7×10^{10} cm^{-2}, which is about 75% of the expected values. High-resolution STEM images shown in the insets of Figs. 1(a) and 1(b) indicate the diameter of columnar defects is ~7 nm, which is slightly larger than those in 2.6-GeV U-irradiated $CaKFe_4As_4$ and K-doped $BaFe_2As_2$ [33–35]. The distribution of these columnar defects is random, and some of them nearly overlap each other, which increases the vortex-vortex interactions and has an important effect on their vortex pinning behavior.

Figures 2(a) and 2(b) illustrate the normalized resistance ($R(T)/R(300\ K)$) versus temperature curves for CsV_3Sb_5 and $Cs(V_{0.93}Nb_{0.07})_3Sb_5$, respectively, under different conditions of U irradiation. The T_c is the onset superconducting transition temperature, which is determined by a 90% criterion of the resistivity. T_{CDW} is determined by the maximum of $dR(T)/dT$. For CsV_3Sb_5, the onset T_c is about 3.2 K, while a clear kink is observed in the R-T curve at ~87 K, which corresponds to the CDW transition. The T_c value of CsV_3Sb_5 initially increases with increasing irradiation dose and reaches the maximum value of ~4.3 K at $B_\Phi = 2.0$ T. However, the T_c value is suppressed to ~3.9 and ~2.3 K for $B_\Phi = 6.0$ and 8.0 T, respectively. The dependence of T_c on B_Φ is similar to that of 2.5 MeV electron-irradiated $NbSe_2$ single crystals, where it is initially enhanced after electron irradiation and then followed by monotonic decline with further increase of irradiation dose [27]. Figure 2(c) shows the temperature dependence of normalized magnetic susceptibility for U-irradiated CsV_3Sb_5, and the data confirmed the results obtained by R-T measurements as shown in the inset of Fig. 2(a). For $Cs(V_{0.93}Nb_{0.07})_3Sb_5$, T_c remains almost unchanged up to $B_\Phi = 2.0$ T, followed by suppression at higher doses as shown in Figs. 2(b) and 2(d).

In order to give a comparison, the superconducting transition temperatures determined by the M-T data marked as $T_c(M)$ are also shown in Fig. 3(a). It is well known that there is a delicate competition between the superconductivity and CDW order in CsV_3Sb_5. Generally speaking, the superconductivity can be enhanced upon suppression of CDW by external perturbation [36]. However, in the present case of CsV_3Sb_5, while the T_c increases up to 4.3 K at a dose of $B_\Phi = 2$ T, the CDW transition temperature (T_{CDW}) is initially enhanced up to ~94 K after U irradiation with $B_\Phi = 0.1$ T and then keeps a nearly constant value at $B_\Phi < 1.0$ T until it is strongly suppressed at large enough B_Φ as shown in Fig. 3(a). Accompanied by enhanced T_c, the value of the residual resistivity ratio (RRR) almost monotonically increases from ~15 to 77 as B_Φ is increased from 0 to 1.0 T and then decreases continuously with further increase of B_Φ, which is different from the report in Refs. [28,29,37]. It has been reported that CsV_3Sb_5 has conventional s-wave pairing with a nodeless superconducting gap [28,38,39]. Therefore, T_c is expected to be insensitive to the disorder in CsV_3Sb_5 according to Anderson's theorem [40]. Recently, Zhang *et al.* systematically investigated the effect of disorder on T_c and T_{CDW} of CsV_3Sb_5, confirming the facts that both T_c and T_{CDW} are insensitive to disorder [41]. Thus, it is reasonable to infer that the enhancement of T_c and T_{CDW} in the present CsV_3Sb_5 crystals has also a weak dependence on disorder. The reason why the values of RRR, T_{CDW}, and T_c increase after small doses of U irradiation is still unclear. One possible reason is the structural relaxation of the crystals after U irradiation.

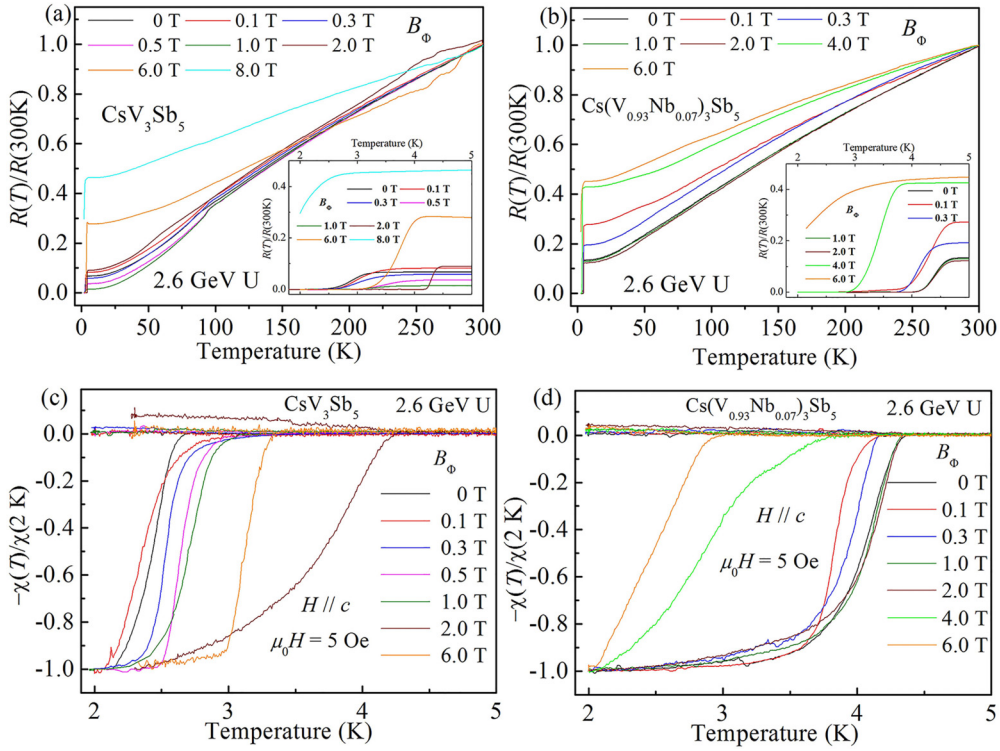

FIG. 2. Temperature dependence of normalized resistance $R(T)/R(300\ \mathrm{K})$ for (a) CsV_3Sb_5 and (b) $Cs(V_{0.93}Nb_{0.07})_3Sb_5$ with different conditions. Insets: The corresponding magnifications of superconducting transition at temperatures close to T_c. The temperature dependence of normalized magnetic susceptibility for (c) CsV_3Sb_5 and (d) $Cs(V_{0.93}Nb_{0.07})_3Sb_5$.

It has been reported that the Debye temperature (Θ_D) of CsV_3Sb_5 crystals is about 160 K, which is even smaller than that of $NbSe_2$ with $\Theta_D \sim 225$ K [42,43]. Thus, the observation is expected of a much stronger dependence of lattice parameter on irradiation dose in CsV_3Sb_5 crystals than that in $NbSe_2$ due to much smaller elastic constant. Figure 4(a) shows the evolution of the diffraction peak of (004) versus the irradiation dose for CsV_3Sb_5 crystals. The x-ray diffraction (XRD) pattern in a broad angle range is shown in Fig. S1 of the Supplemental Material [44]. It can be seen that diffraction angle increases slightly with increasing irradiation dose. The corresponding values of the c-axis lattice parameter shrink with increasing irradiation dose as shown in Fig. 4(b). The change of c-axis lattice parameter versus B_Φ is approximately linear up to $B_\Phi = 8$ T, and the corresponding strain is about -0.11%. However, the c-B_Φ curve strongly deviates from linearity above $B_\Phi = 8$ T as shown in Fig. 4(b). It is well known that the lattice constant generally increases with the introduction of defects [45]. In this sense, shrinkage of the c-axis lattice parameter is anomalous. Recently, Yang *et al.* have pointed out that in-plane uniaxial-strain tuning of T_c in CsV_3Sb_5 is dominated by associated c-axis strain [46]. However, the calculated strain is only about -0.006% along the c axis for CsV_3Sb_5 crystals after 2.6-GeV U irradiations with $B_\Phi \sim 2$ T. The strain is too small to explain the remarkable enhancement of T_c. Another possible explanation

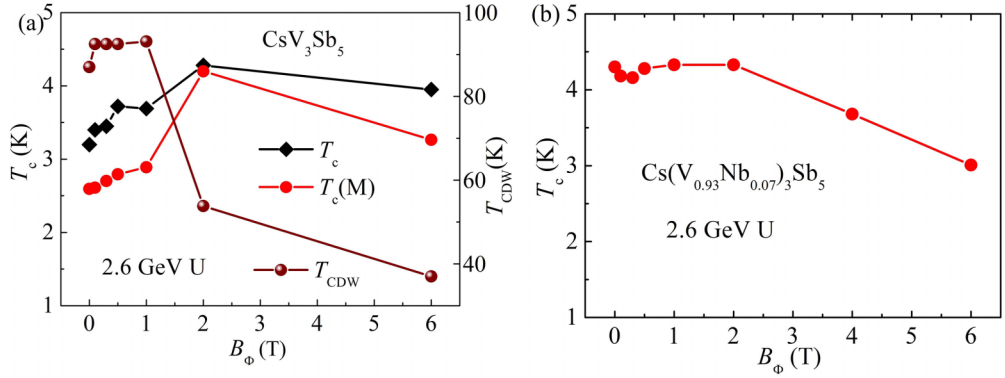

FIG. 3. (a) Irradiation dose (B_Φ) dependence of T_c and T_{CDW} for CsV_3Sb_5 and (b) irradiation dose (B_Φ) dependence of T_c for $Cs(V_{0.93}Nb_{0.07})_3Sb_5$.

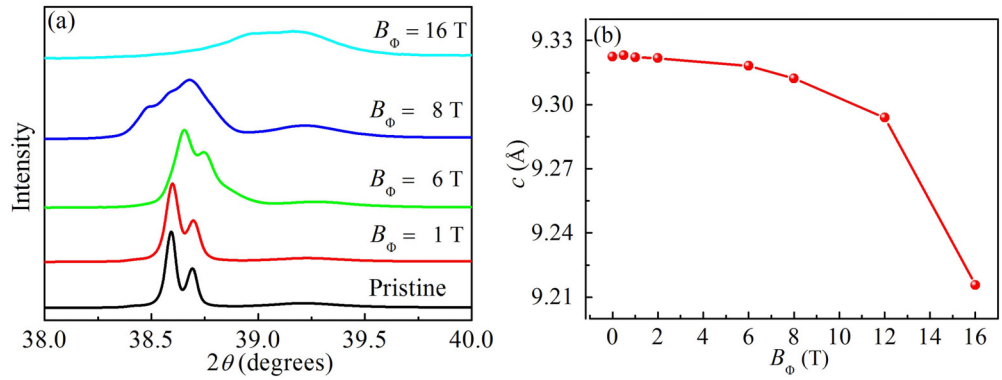

FIG. 4. (a) The XRD pattern of (004) peaks and (b) the curve of c-axis lattice parameters versus B_Φ for CsV_3Sb_5 single crystals with 2.6-GeV U irradiation.

could be due to the slight oxidation (hole doping) of the material triggered by absorption of oxygen on the surface. In Ref. [24], systematic changes of physical properties, including the enhancement of T_c and suppression of T_{CDW}, due to surface oxidation have been demonstrated by studying CsV_3Sb_5 crystals with different thicknesses down to 12 nm. Usually, the effect of such hole doping is restricted only to the surface of the crystal. However, since the resistivity in the defect region is expected to increase significantly, introduced surface charge by oxidation can also modify the carrier density in the bulk of the crystal. In this case, the density of states and nesting of the Fermi surface can be changed [24]. The excessive reduction of the c-axis lattice parameter at large irradiation doses can be attributed to the electronic excitation, resulting in producing additional defects [47]. It has been reported that the interplay between the CDW and superconductivity in the AV_3Sb_5 (A = K, Rb, Cs) system is not simply a competition for the density of states near the Fermi level, and the electronic correlations also play an important role in manipulating the CDW and its entanglement with superconductivity [48]. In addition, the initial increase of RRR after 2.6-GeV U irradiation can also be originated from the hole doping into the bulk.

Figures 5(a) and 5(b) show the temperature dependence of normalized resistance ($R(T)/R(5\ K)$) for the U-irradiated CsV_3Sb_5 and $Cs(V_{0.93}Nb_{0.07})_3Sb_5$ with $B_\Phi = 2.0$ T under different magnetic fields ($H \| c$), respectively. As we have already mentioned above, the superconductivity for CsV_3Sb_5 is greatly enhanced upon U irradiation, and the superconductivity is observed above 2.0 K even at a high magnetic field of 1.5 T. For $Cs(V_{0.93}Nb_{0.07})_3Sb_5$, the superconductivity is robust and no clear decay is observed at B_Φ less than 2.0 T. The superconducting transition is very sharp, which is similar to low-T_c conventional superconductors, and "122" and "1144" iron-based superconductors [49–51], indicating small thermal fluctuations as shown in Figs. 5(a) and 5(b). As a comparison, the curves of $R(T)/R(5\ K)$ versus temperature for CsV_3Sb_5 and $Cs(V_{0.93}Nb_{0.07})_3Sb_5$ with $B_\Phi = 0.3$ T are shown by Figs. S2(a) and S2(b), respectively, of the Supplemental Material [44]. The upper critical fields, H_{c2}, were evaluated following the Ginzburg-Landau theory of $H_{c2} = H_{c2}(0)(1 - t^2)/(1 + t^2)$ by using the criterion of $R = 0.5R_n$, where R_n and t are the normal state resistance just above T_c and the reduced temperature ($t = T/T_c$), respectively. The evaluated values of $H_{c2}(0)$ for CsV_3Sb_5 and $Cs(V_{0.93}Nb_{0.07})_3Sb_5$ with $B_\Phi = 2.0$ T are 1.9 and 2.2 T, respectively. The corresponding coherence lengths $\xi_{ab}(0)$ are 13 and 12 nm, respectively. These lengths are more than five times larger than that of iron-based and cuprate superconductors [52].

Figures 5(c) and 5(d) show the magnetic hysteresis loops (MHLs) for CsV_3Sb_5 and $Cs(V_{0.93}Nb_{0.07})_3Sb_5$ irradiated by 2.6-GeV U at $B_\Phi = 2.0$ T, respectively. MHLs for samples with other B_Φ are shown by Figs. S3 and S4 of the Supplemental Material [44]. The symmetric shape of the MHL for the irradiated $Cs(V_{0.93}Nb_{0.07})_3Sb_5$ suggests that bulk pinning instead of surface pinning is in charge of vortex pinning in this sample. For CsV_3Sb_5, the widths of MHLs initially become larger with increasing irradiation dose and reach the maximum value at $B_\Phi \sim 1.0$ T, and decline by further increase of B_Φ as shown in Figs. S3 of the Supplemental Material [44] and Fig. 5(c). For easy comparison, the MHL for pristine CsV_3Sb_5 is also shown by Fig. S5 of the Supplemental Material [44]. In addition, no peak effect is observed in CsV_3Sb_5. This is clearly different from the proton-irradiated CsV_3Sb_5 in which a broad peak was observed at intermediate fields [29]. The central peak near zero field for CsV_3Sb_5 is sharp even after U irradiation, unlike the case of $Ba(Fe_{0.93}Co_{0.07})_2As_2$ irradiated by 200-MeV Au where the magnetization peak near zero field is broad [53]. For $Cs(V_{0.93}Nb_{0.07})_3Sb_5$, symmetric MHLs and similar changing tendency with increasing magnetic fields are observed. In contrast to CsV_3Sb_5, one prominent feature is that a dip structure near zero field is observed at low B_Φ as shown in Fig. 7(a) and Fig. S4 of the Supplemental Material [44], which is similar to the iron-based superconductors, cuprate superconductors, and $NbSe_2$ after introduction of columnar defects [30,54–56].

Figures 6(a) and 6(b) illustrate the irradiation dose dependence of J_c under the self-field at various temperatures in CsV_3Sb_5 and $Cs(V_{0.93}Nb_{0.07})_3Sb_5$. For CsV_3Sb_5, the J_c displays different tendencies with increasing B_Φ at different temperatures. For example, at 2.3 K, the J_c initially increases with increasing B_Φ and decreases at B_Φ larger than 1.0 T, while it increases monotonically with increasing B_Φ at temperatures above 2.6 K. One reasonable reason for such behavior is that the U irradiation induces δT_c pinning in CsV_3Sb_5, which is very effective at temperatures close to T_c. Here δT_c pinning is defined as flux pinning induced by spatial fluctuations of the superconducting transition temperature T_c. The J_c value is about 0.8×10^4 A/cm^2 for CsV_3Sb_5 at

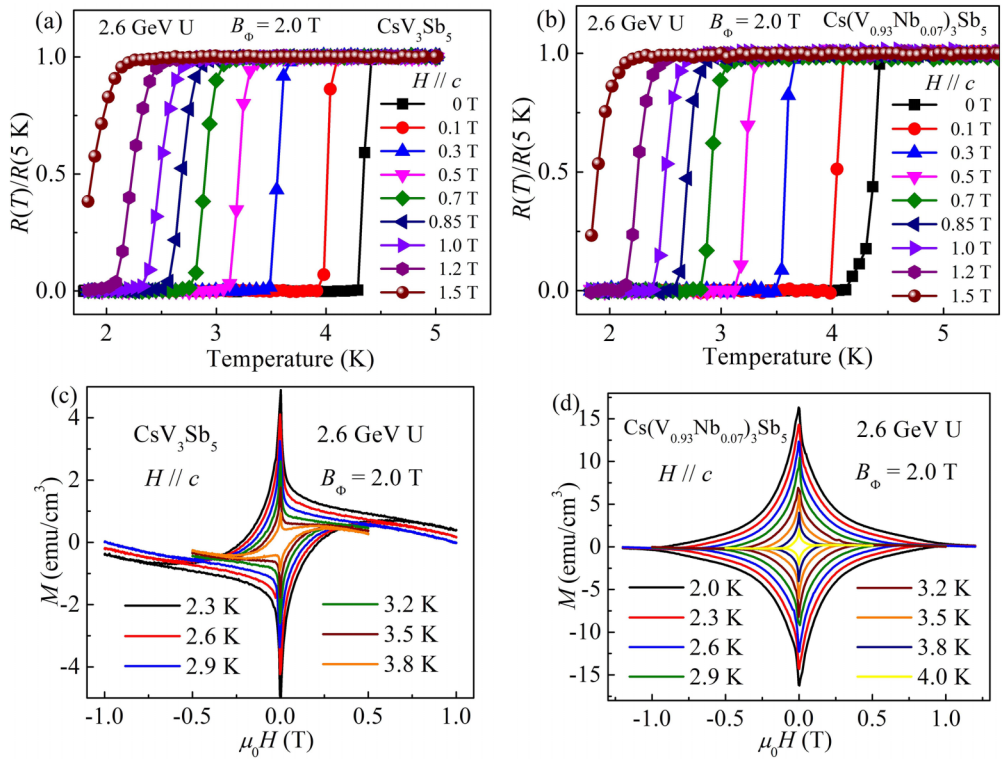

FIG. 5. Temperature dependence of normalized resistance $R(T)/R(5\ \mathrm{K})$ under different magnetic fields for (a) CsV_3Sb_5 and (b) $Cs(V_{0.93}Nb_{0.07})_3Sb_5$, at $B_\Phi = 2.0$ T. MHLs under different temperatures for (c) CsV_3Sb_5 and (d) $Cs(V_{0.93}Nb_{0.07})_3Sb_5$, at $B_\Phi = 2.0$ T.

$B_\Phi = 0.5$ T, which is about four times larger than the pristine sample at the same condition. For $Cs(V_{0.93}Nb_{0.07})_3Sb_5$, the J_c initially increases with increasing B_Φ and takes the maximum at about $B_\Phi = 0.5$ T, followed by monotonic decrease above $B_\Phi = 0.5$ T. The B_Φ dependencies of J_c at various temperatures are similar to each other for $Cs(V_{0.93}Nb_{0.07})_3Sb_5$ as shown in Fig. 6(b). The largest value of J_c under the self-field at 2 K for $Cs(V_{0.93}Nb_{0.07})_3Sb_5$ after 2.6-GeV U irradiation is $\sim 2.3 \times 10^4$ A/cm^2 in a sample with $B_\Phi \sim 0.5$ T, which is about 3.5 times larger than the pristine sample [29]. It should be noted that the J_c values in 2.6-GeV U-irradiated CsV_3Sb_5 and $Cs(V_{0.93}Nb_{0.07})_3Sb_5$ are several orders of magnitude smaller than that in cuprates ($J_c(5\ \mathrm{K}) \sim 1.35 \times 10^7$ A/cm^2, 580 MeV Sn, $B_\Phi = 3$ T) [57] and iron-based superconductors ($J_c(2\ \mathrm{K}) \sim 1.4 \times 10^7$ A/cm^2, 2.6 GeV U, $B_\Phi = 8$ T) [33], indicating that pinning in kagome superconductors is weak. One possible reason is that the typical diameter of columnar defects (~7 nm) created by heavy-ion irradiation is much smaller than the coherence length of ~20 nm, making the flux pinning less effective [58]. Generally, different defect structures (pointlike, cluster, columnar, etc.) have different effects at different field and current values, and a mix of defect types may give the best pinning effect [59].

Figure 7(a) shows MHLs for $Cs(V_{0.93}Nb_{0.07})_3Sb_5$ irradiated by 2.6-GeV U ions at $B_\Phi = 0.2$ T at various temperatures. It is clear that anomalous peak structures develop close to zero field at low temperatures. Similar peak structures can be observed in a sample irradiated at $B_\Phi = 0.1$ T at low temperatures as shown in Fig. S4(a) of the Supplemental Material [44]. The peak structure gradually

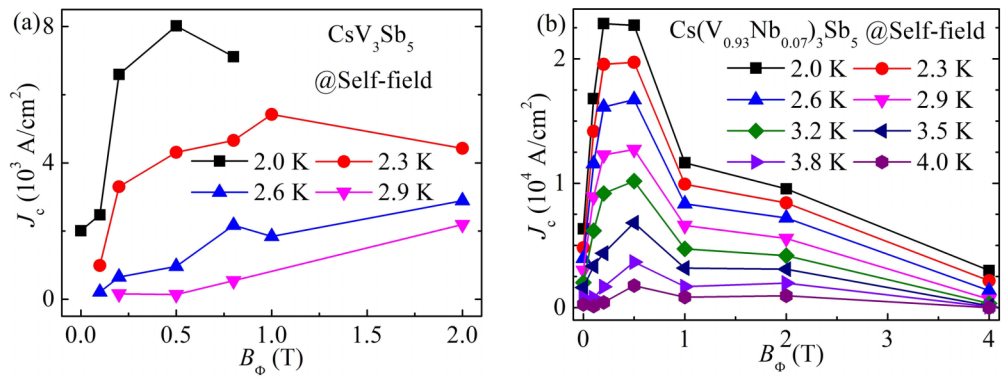

FIG. 6. The curves of J_c versus B_Φ under self-field and various temperatures for (a) CsV_3Sb_5 and (b) $Cs(V_{0.93}Nb_{0.07})_3Sb_5$.

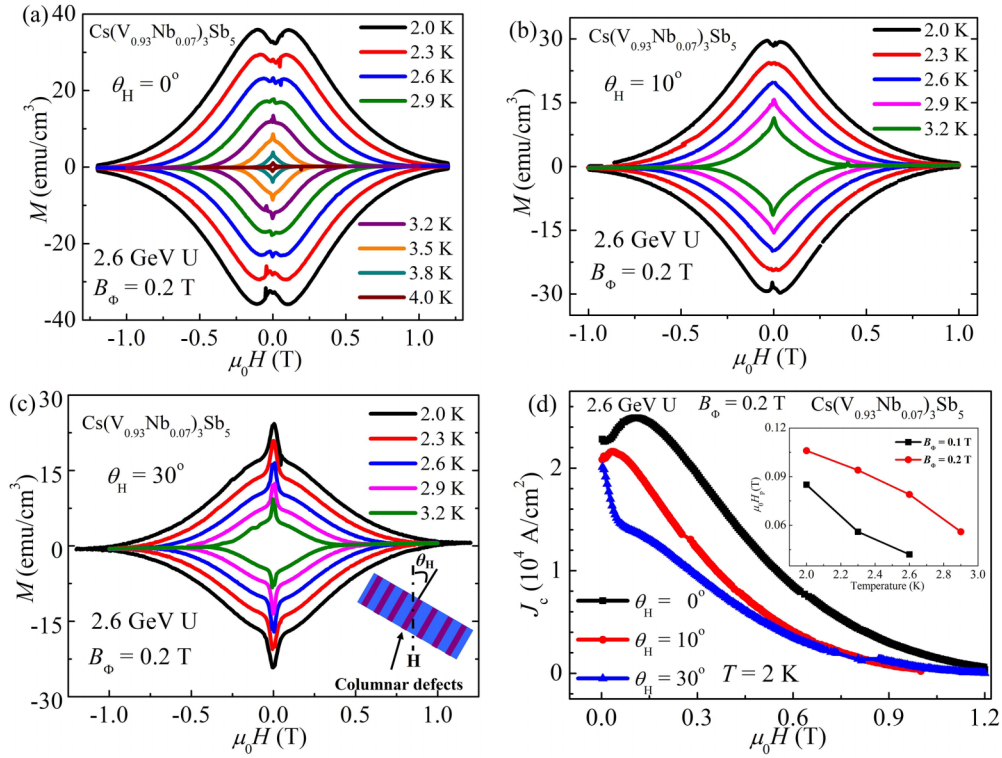

FIG. 7. *M*-*H* loops at various temperatures for 2.6-GeV U-irradiated $Cs(V_{0.93}Nb_{0.07})_3Sb_5$ with $B_\Phi = 0.2$ T at (a) $\theta_H = 0°$, (b), $\theta_H = 10°$, and (c) $\theta_H = 30°$. (d) The J_c versus H curves at different θ_H angles at $T = 2.0$ K. The inset of (c) shows a schematic diagram explaining θ_H as the angle between the columnar defects and the applied fields H. The inset of (d) shows temperature dependence of $\mu_0 H_p$ for $Cs(V_{0.93}Nb_{0.07})_3Sb_5$ with $B_\Phi = 0.1$ and 0.2 T.

fades away with increasing B_Φ above $B_\Phi = 0.2$ T as shown in Figs. S4(b)–S4(d) [44]. Such abnormal magnetization behavior has also been observed in heavy-ion irradiated high-T_c cuprates [60], $NbSe_2$, and iron-based superconductors [61]. For instance, peak effects located close to $\mu_0 H = B_\Phi/3$ have been observed in $YBa_2Cu_3O_7$ irradiated by 580-MeV Sn ions and in $Ba_{1-x}K_xFe_2As_2$ irradiated by 2.6-GeV U ions [33], and dips near zero field in MHLs have been observed in $Ba(Fe_{0.93}Co_{0.07})_2As_2$ irradiated with 2.6-GeV U ions [30]. For the present U-irradiated $Cs(V_{0.93}Nb_{0.07})_3Sb_5$ with $B_\Phi =$ 0.1 and 0.2 T, the peak field ($\mu_0 H_p$) locates at $\sim 0.55 B_\Phi$ at 2 K, which decreases with increasing temperature and finally merges into the central magnetization peak. The peak field $\mu_0 H_p$ is about 0.06 and 0.11 T at 2.0 K for the U-irradiated samples with $B_\Phi = 0.1$ and 0.2 T, respectively. These values of $\mu_0 H_p$ are much larger than the self-field of $\mu_0 H_{sf}$, $\sim$0.004 and 0.012 T for $B_\Phi = 0.1$ and 0.2 T samples, respectively. Thus, it is unlikely that the present peak structure is caused by the self-field effect. Specific arrangements of columnar defects can be classified into three types, namely, parallel columnar defects (columnar defects parallel to the c axis), tilted columnar defects (columnar defects tilted from the c axis), and bimodal splayed columnar defects (columnar defects are tilted symmetrically from the c axis). In superconductors with parallel columnar defects, peak effects which have similar shapes to those observed in the present study have not been observed [62]. On the other hand, in superconductors with tilted columnar defects [57,63] and splayed columnar defects [33,56,64], similar peak effects have been observed at fields close to αB_Φ with $0.1 < \alpha < 0.3$. In the present case, $\mu_0 H_p$ is closer to B_Φ, suggesting that it is caused by the matching effect.

When a regular array of pinning centers is introduced into superconductors, the pinning force density reaches the maximum value when all pinning centers are occupied by vortices. On the other hand, when the arrangement of pinning centers is random as in the case of columnar defects created by heavy-ion irradiations, the optimum pinning can be realized before all pinning centers are occupied by vortices due to the competition between pinning energy and vortex-vortex interactions. However, even in superconductors with randomly distributed pinning centers, when the vortex-vortex interaction is not strong enough, the maximum pinning force density is reached when the applied magnetic field (H) is close to B_Φ, namely, $\mu_0 H/B_\Phi \sim 1$ [56]. In the present case of U-irradiated $Cs(V_{0.93}Nb_{0.07})_3Sb_5$ crystals, although the exact value of the penetration depth is not known, it is expected to be shorter than that for the pristine material of 387 nm [28], making vortex-vortex interactions weaker and $\mu_0 H_p/B_\Phi \sim 0.55$. At higher temperatures, as the penetration depth becomes longer, the optimum pinning is realized at lower applied fields as observed in the inset of Fig. 7(d) [58,65,66].

Figures 7(b) and 7(c) show the MHL when the external field is applied at $\theta_H = 10°$ and 30° from the c axis, respectively. Figure 7(d) shows the magnetic field dependence of J_c at 2.0 K at different θ_H. It is clear that the peak structure becomes weaker by titling the external field away from the columnar defects. At $\theta_H = 10°$, the peak structure becomes

less pronounced, and nearly normal field dependence of J_c with a weak hump at 0.15 T is observed at $\theta_H = 30^\circ$. Another important feature of the peak structure is that it fades away with increasing temperature. Due to the increase of the coherence length ξ(T) with increasing temperature, the pinning by columnar defects becomes weaker. As a result, the peak structure fades away as shown in Fig. 7(a). It should be noted that similar peak structures are not observed in CsV_3Sb_5 after 2.6-GeV U irradiation at $T = 2.0$ K. One possible reason is that the measuring temperature of 2.0 K is too close to its T_c so that the dip structure is not developed, similar to the case of 2.6-GeV U-irradiated $Cs(V_{0.93}Nb_{0.07})_3Sb_5$ at high temperatures.

IV. CONCLUSIONS

In summary, we have studied the effect of 2.6-GeV U irradiation on the superconductivity of CsV_3Sb_5 and $Cs(V_{0.93}Nb_{0.07})_3Sb_5$ single crystals. We observe that the c-axis lattice parameter shrinks after irradiation. Besides the enhancement of J_c, the T_c is enhanced up to ∼4.3 K after U irradiation at $B_\Phi = 2.0$ T in CsV_3Sb_5. By contrast, the T_c value for the 2.6-GeV U-irradiated $Cs(V_{0.93}Nb_{0.07})_3Sb_5$ initially keeps a high value of ∼4.3 K at B_Φ less than 2.0 T, followed by monotonic decrease with further increase of the irradiation dose. Upon 2.6-GeV U irradiation, the J_c in $Cs(V_{0.93}Nb_{0.07})_3Sb_5$ is enhanced up to $\sim 2.3 \times 10^4$ A/cm^2 under the self-field at $T = 2.0$ K, which is about 3.5 times larger than that in the pristine sample at the same condition. We observe peak structures in irreversible magnetization loops at low fields only in $Cs(V_{0.93}Nb_{0.07})_3Sb_5$ irradiated by 2.6-GeV U ions at $B_\Phi < 0.5$ T. Although the peak structure has some similarity to the self-field peak effect observed in iron-based superconductors with columnar defects along the c axis, the peak field is about ten times larger than the self-field, and is close to B_Φ. A matching effect of vortices with the density of columnar defects affected by weaker vortex-vortex interactions due to temperature-dependent penetration depth can be an alternative explanation.

ACKNOWLEDGMENTS

This work has been supported by the China Scholarship Council (CSC), the Natural Science Foundation of the Henan province of China (Grant No. 242300421395). The work at the Beijing Institute of Technology was supported by the National Natural Science Foundation of China (Grant No. 92065109), and the Beijing Natural Science Foundation (Grant No. Z210006).

[1] M. Fu, T. Imai, T. H. Han, and Y. S. Lee, Evidence for a gapped spin-liquid ground state in a kagome Heisenberg antiferromagnet, Science **350**, 655 (2015).

[2] L. Ye, M. Kang, J. Liu, F. Cube, C. R. Wicker, T. Suzuki, C. Jozwiak, A. Bostwick, E. Rotenberg, D. C. Bell, L. Fu, R. Comin, and J. G. Checkelsky, Massive Dirac fermions in a ferromagnetic kagome metal, Nature (London) **555**, 638 (2018).

[3] E. Liu, Y. Sun, N. Kumar, L. Muechler, A. Sun, L. Jiao, S. Yang, D. Liu, A. Liang, Q. Xu, J. Kroder, V. Süß, H. Borrmann, C. Shekhar, Z. Wang, C. Xi, W. Wang, W. Schnelle, S. Wirth, Y. Chen, S. T. B. Goennenwein, and C. Felser, Giant anomalous Hall effect in a ferromagnetic kagome-lattice semimetal, Nat. Phys. **14**, 1125 (2018).

[4] W.-S. Wang, Z.-Z. Li, Y.-Y. Xiang, and Q.-H. Wang, Competing electronic orders on kagome lattice at van Hove filling, Phys. Rev. B **87**, 115135 (2013).

[5] H. M. Guo and M. Franz, Topological insulator on the kagome lattice, Phys. Rev. B **80**, 113102 (2009).

[6] W. H. Ko, P. A. Lee, and X. G. Wen, Doped kagome system as exotic superconductor, Phys. Rev. B **79**, 214502 (2009).

[7] S. Yan, D. A. Huse, and S. R. White, Spin-liquid ground state of the $S = 1/2$ kagome Heisenberg antiferromagnet, Science **332**, 1173 (2011).

[8] S. L. Yu and J. X. Li, Chiral superconducting phase and chiral spin-density-wave phase in a Hubbard model on the kagome lattice, Phys. Rev. B **85**, 144402 (2012).

[9] B. R. Ortiz, S. M. L. Teicher, Y. Hu, J. L. Zuo, P. M. Sarte, E. C. Schueller, A. M. M. Abeykoon, M. J. Krogstad, S. Rosenkranz, R. Osborn, R. Seshadri, L. Balents, J. He, and S. D. Wilson, CsV_3Sb_5: A $\mathbb{Z}_2$ topological kagome metal with a superconducting ground state, Phys. Rev. Lett. **125**, 247002 (2020).

[10] B. R. Ortiz, L. C. Gomes, J. R. Morey, M. Winiarski, M. Bordelon, J. S. Mangum, I. W. H. Oswald, J. A. Rodriguez-Rivera, J. R. Neilson, S. D. Wilson, E. Ertekin, T. M. McQueen, and E. S. Toberer, New kagome prototype materials: Discovery of KV_3Sb_5, RbV_3Sb_5, and CsV_3Sb_5, Phys. Rev. Mater. **3**, 094407 (2019).

[11] Q. Yin, Z. Tu, C. Gong, Y. Fu, S. Yan, and H. Lei, Superconductivity and normal-state properties of kagome metal RbV_3Sb_5 single crystals, Chin. Phys. Lett. **38**, 037403 (2021).

[12] Y. Xiang, Q. Li, Y. Li, W. Xie, H. Yang, Z. Wang, Y. Yao, and H. H. Wen, Twofold symmetry of c-axis resistivity in topological kagome superconductor CsV_3Sb_5 with in-plane rotating magnetic field, Nat. Commun. **12**, 6727 (2021).

[13] L. Nie, K. Sun, W. Ma, D. Song, L. Zheng, Z. Liang, P. Wu, F. Yu, J. Li, M. Shan, D. Zhao, S. Li, B. Kang, Z. Wu, Y. Zhou, K. Liu, Z. Xiang, J. Ying, Z. Wang, T. Wu, and X. Chen, Charge-density-wave-driven electronic nematicity in a kagome superconductor, Nature (London) **604**, 59 (2022).

[14] F. H. Yu, T. Wu, Z. Y. Wang, B. Lei, W. Z. Zhuo, J. J. Ying, and X. H. Chen, Concurrence of anomalous Hall effect and charge density wave in a superconducting topological kagome metal, Phys. Rev. B **104**, L041103 (2021).

[15] S. Y. Yang, B. R. Ortiz Y.Wang, D. Liu, J. Gayles, E. Derunova, R. Gonzalez-Hernandez, L. Šmejkal, Y. Chen, S. S. P. Parkin, S. D. Wilson, E. S. Toberer, T. McQueen, and M. N. Ali, Giant, unconventional anomalous Hall effect in the metallic frustrated magnet candidate, KV_3Sb_5, Sci. Adv. **6**, eabb6003 (2020).

[16] B. R. Ortiz, S. M. L. Teicher, L. Kautzsch, P. M. Sarte, N. Ratcliff, J. Harter, J. P. C. Ruff, R. Seshadri, and S. D. Wilson, Fermi surface mapping and the nature of charge-density-wave order in the kagome superconductor CsV_3Sb_5, Phys. Rev. X **11**, 041030 (2021).

[17] G. L. Zheng, C. Tan, Z. Chen, M. Y. Wang, X. D. Zhu, S. Albarakati, M. Algarni, J. Partridge, L. Farrar, J. H. Zhou, W. Ning, M. L. Tian, M. S. Fuhrer, and L. Wang, Electrically controlled superconductor-to-failed insulator transition and giant anomalous Hall effect in kagome metal CsV_3Sb_5 nanoflakes, Nat. Commun. **14**, 678 (2023).

[18] Y. M. Oey, B. R. Ortiz, F. Kaboudvand, J. Frassineti, E. Garcia, R. Cong, S. Sanna, V. F. Mitrović, R. Seshadri, and S. D. Wilson, Fermi level tuning and double-dome superconductivity in the kagome metal $CsV_3Sb_{5-x}Sn_x$, Phys. Rev. Mater. **6**, L041801 (2022).

[19] L. Kautzsch, Y. M. Oey, H. Li, Z. Ren, B. R. Ortiz, G. Pokharel, R. Seshadri, J. Ruff, T. Kongruengkit, J. W. Harter, Z. Q.Wang, I. Zeljkovic, and S. D. Wilson, Incommensurate charge-stripe correlations in the kagome superconductor $CsV_3Sb_{5-x}Sn_x$, npj Quantum Mater. **8**, 37 (2023).

[20] H. Yang, Z. Huang, Y. Zhang, Z. Zhao, J. Shi, H. Luo, L. Zhao, G. Qian, H. Tan, B. Hu, K. Zhu, Z. Lu, H. Zhang, J. Sun, J. Cheng, C. Shen, X. Lin, B. Yan, X. Zhou, Z. Wang *et al.*, Titanium doped kagome superconductor $CsV_{3-x}Ti_xSb_5$ and two distinct phases, Sci. Bull. **67**, 2176 (2022).

[21] J. Y. L. Li, W. Xie, J. J. Liu, Q. Li, X. Li, H. Yang, Z. W. Wang, Y. G. Yao, and H. H. Wen, Strong-coupling superconductivity and weak vortex pinning in Ta-doped CsV_3Sb_5 single crystals, Phys. Rev. B **106**, 214529 (2022).

[22] Y. K. Li, Q. Li, X. W. Fan, J. J. Liu, Q. Feng, M. Liu, C. L. Wang, J. X. Yin, J. X. Duan, X. Li, Z. W. Wang, H. H. Wen, and Y. G. Yao, Tuning the competition between superconductivity and charge order in the kagome superconductor $Cs(V_{1-x}Nb_x)_3Sb_5$, Phys. Rev. B **105**, L180507 (2022).

[23] Y. Liu, C. C. Liu, Q. Q. Zhu, L. W. Ji, S. Q. Wu, Y. L. Sun, J. K. Bao, W. H. Jiao, X. F. Xu, Z. Ren, and G. H. Cao, Enhancement of superconductivity and suppression of charge-density wave in As-doped CsV_3Sb_5, Phys. Rev. Mater. **6**, 124803 (2022).

[24] Y. P. Song, T. P. Ying, X. Chen, X. Han, X. X. Wu, A. P. Schnyder, Y. Huang, J. G. Guo, and X. L. Chen, Competition of superconductivity and charge density wave in selective oxidized CsV_3Sb_5 thin flakes, Phys. Rev. Lett. **127**, 237001 (2021).

[25] K. Y. Chen, N. N. Wang, Q. W. Yin, Y. H. Gu, K. Jiang, Z. J. Tu, C. S. Gong, Y. Uwatoko, J. P. Sun, H. C. Lei, J. P. Hu, and J. G. Cheng, Double superconducting dome and triple enhancement of T_c in the kagome superconductor CsV_3Sb_5 under high pressure, Phys. Rev. Lett. **126**, 247001 (2021).

[26] Q. Wang, P. F. Kong, W. J. Shi, C. Y. Pei, C. H. P. Wen, L. L. Gao, Y. Zhao, Q. W. Yin, Y. S.Wu, G. Li, H. C. Lei, J. Li, Y. L. Chen, S. C. Yan, and Y. P. Qi, Charge density wave orders and enhanced superconductivity under pressure in the kagome metal CsV_3Sb_5, Adv. Mater. **33**, 2102813 (2021).

[27] K. Cho, M. Konczykowski, S. Teknowijoyo, M. A. Tanatar, J. Guss, P. Gartin, J. M. Wilde, A. Kreyssig, R. McQueeney, A. I. Goldman, V. Mishra, P. J. Hirschfeld, and R. Prozorov, Using controlled disorder to probe the interplay between charge order and superconductivity in $NbSe_2$, Nat. Commun. **9**, 2796 (2018).

[28] M. Roppongi, K. Ishihara, Y. Tanaka, K. Ogawa, K. Okada, S. Liu, K. Mukasa, Y. Mizukami, Y. Uwatoko, R. Grasset, M. Konczykowski, B. R. Ortiz, S. D. Wilson, K. Hashimoto, and T. Shibauchi, Bulk evidence of anisotropic *s*-wave pairing with no sign change in the kagome superconductor CsV_3Sb_5, Nat. Commun. **14**, 667 (2023).

[29] C. L. Wang, Y. Hirota, L. B. Wang, R. Sakagami, Y. K. Li, X. L. Yi, W. J. Li, Y. S. Chen, C. Yu, Z. W. Wang, and T. Tamegai, Peak effects in the kagome superconductors CsV_3Sb_5 and $Cs(V_{0.93}Nb_{0.07})_3Sb_5$, Phys. Rev. B **109**, 024514 (2024).

[30] T. Tamegai, T. Taen, H. Yagyuda, Y. Tsuchiya, S. Mohan, T. Taniguchi, Y. Nakajima, S. Okayasu, M. Sasase, H. Kitamura, T. Murakami, T. Kambara, and Y. Kanai, Effects of particle irradiation on vortex states in iron-based superconductors, Supercond. Sci. Technol. **25**, 084008 (2012).

[31] T. Taen, F. Ohtake, S. Pyon, T. Tamegai, and H. Kitamura, Critical current density and vortex dynamics in pristine and proton-irradiated $Ba_{0.6}K_{0.4}Fe_2As_2$, Supercond. Sci. Technol. **28**, 085003 (2015).

[32] J. Ziegler, J. Biersack, and U. Littmark, *The Stopping and Range of Ions in Solids* (Pergamon, New York, 1985), p. 202.

[33] A. Park, S. Pyon, K. Ohara, N. Ito, T. Tamegai, T. Kambara, A. Yoshida, and A. Ichinose, Field-driven transition in the $Ba_{1-x}K_xFe_2As_2$ superconductor with splayed columnar defects, Phys. Rev. B **97**, 064516 (2018).

[34] S. Pyon, Y. Kobayashi, A. Takahashi, W. Li, T. Wang, G. Mu, A. Ichinose, T. Kambara, A. Yoshida, and T. Tamegai, Anisotropic physical properties and large critical current density in $KCa_2Fe_4As_4F_2$ single crystal, Phys. Rev. Mater. **4**, 104801 (2020).

[35] A. Takahashi, S. Pyon, Y. Kobayashi, T. Kambara, A. Yoshida, S. Okayasu, A. I. Ichinose, and T. Tamegai, Effects of splayed columnar defects on critical current density in $CaKFe_4As_4$, J. Phys.: Conf. Ser. **1590**, 012015 (2020).

[36] C. C. Zhao, L. S. Wang, W. Xia, Q. W. Yin, J. M. Ni, Y. Y. Huang, C. P. Tu, Z. C. Tao, Z. J. Tu, C. S. Gong, H. C. Lei, Y. F. Guo, X. F. Yang, and S. Y. Li, Nodal superconductivity and superconducting domes in the topological kagome metal CsV_3Sb_5, arXiv:2102.08356.

[37] W. J. Li, S. S. Pyon, A. Yagi, T. Ren, M. Suyama, J. Wang, T. Matsumae, Y. Kobayashi, A. Takahashi, D. Miyawaki, and T. Tamegai, Effects of 3 MeV proton irradiation on superconductivity and CDW in $2H$-$NbSe_2$ single crystals, J. Phys. Soc. Jpn. **92**, 064701 (2023).

[38] C. Mu, Q. W. Yin, Z. J. Tu, C. S. Gong, H. C. Lei, Z. Li, and J. L. Luo, S-wave superconductivity in kagome metal CsV_3Sb_5 revealed by $^{121/123}$Sb NQR and ^{51}V NMR measurements, Chin. Phys. Lett. **38**, 077402 (2021).

[39] W. Y. Duan, Z. Y. Nie, S. S. Luo, F. H. Yu, B. R. Ortiz, L. C. Yin, H. Su, F. Du, A. Wang, Y. Chen, X. Lu, J. J. Ying, S. D. Wilson, X. H. Chen, Y. Song, and H. Q. Yuan, Nodeless superconductivity in the kagome metal CsV_3Sb_5, Sci. China: Phys. Mech. Astron. **64**, 107462 (2021).

[40] P. W. Anderson, Theory of dirty superconductors, J. Phys. Chem. Solids **11**, 26 (1959).

[41] W. Zhang, X. Y. Liu, L. F. Wang, C. W. Tsang, Z. Y. Wang, S. T. Lam, W. Y. Wang, J. Y. Xie, X. F. Zhou, Y. S. Zhao, S. M. Wang, J. Tallon, and K. T. Lai, Nodeless superconductivity in kagome metal CsV_3Sb_5 with and without time reversal symmetry breaking, Nano Lett. **23**, 872 (2023).

[42] J. Yan, L. Shan, Y. Wang, Z.-L. Xiao, and H.-H. Wen, Quasiparticle density of states of $2H$-$NbSe_2$ single crystals revealed by low-temperature specific heat measurements according to a two-component model, Chinese Phys. B **17**, 2229 (2008).

[43] K. Y. Yang, W. Xia, X. R. Mi, L. Zhang, Y. H. Gan, A. F. Wang, Y. S. Chai, X. Y. Zhou, X. L. Yang, Y. F. Guo, and M. Q. He,

Charge fluctuations above T_{CDW} revealed by glasslike thermal transport in kagome metals AV_3Sb_5 (A = K, Rb, Cs), Phys. Rev. B **107**, 184506 (2023).

[44] See Supplemental Material at http://link.aps.org/supplemental/10.1103/PhysRevB.110.054520 for the data on XRD patterns, temperature dependence of normalized resistivity $R(T)/R(5\ \mathrm{K})$, magnetization hysteresis loops, and the curve of critical current density versus magnetic fields.

[45] W. J. Li, S. Pyon, A. Ichinose, S. Okayasu, and T. Tamegai, Suppression of superconductivity in heavy-ion irradiated $2H$-$NbSe_2$ caused by negative pressure, J. Phys. Soc. Jpn. **91**, 074709 (2022).

[46] X. R. Yang, Q. Tang, Q. Y. Zhou, H. P. Wang, Y. Li, X. Fu, J. W. Zhang, Y. Song, H. Q. Yuan, P. C. Dai, and X. Y. Lu, In-plane uniaxial-strain tuning of superconductivity and charge-density wave in CsV_3Sb_5, Chin. Phys. B **32**, 127101 (2023).

[47] N. Ishikawa, A. Iwase, Y. Chimi, H. Maeta, K. Tsuru, and O. Michikami, Lattice expansion in $EuBa_2Cu_3O_y$ irradiated with energetic ions, Physica C **259**, 54 (1996).

[48] X. X. Zhou, Y. K. Li, X. W. Fan, J. H. Hao, Y. Xiang, Z. Liu, Y. M. Dai, Z. W. Wang, Y. G. Yao, and H. H. Wen, Phys. Rev. B **107**, 165123 (2023).

[49] X. L. Wang, S. R. Ghorbani, S. Lee, S. X. Dou, C. T. Lin, T. H. Johansen, K. H. Müller, Z. X. Cheng, G. Peleckis, M. Shabazi, A. J. Qviller, V. V. Yurchenko, G. L. Sun, and D. L. Sun, Very strong intrinsic flux pinning and vortex avalanches in (Ba, K)Fe_2As_2 superconducting single crystals, Phys. Rev. B **82**, 024525 (2010).

[50] W. N. Kang, H. Kim, E. Choi, C. U. Jung, and S. Lee, MgB_2 superconducting thin film with a transition temperature of 39 Kelvin, Science **292**, 1521 (2001).

[51] C. L. Wang, T. He, Q. Q. Han, B. Z. Wang, R. H. Xie, Y. G. Li, Q. B. Tang, Y. B. Li, and B. H. Yu, Flux pinning and the vortex phase diagram in optimized $CaKFe_4As_4$ single crystals fabricated by a one-step method, Supercond. Sci. Technol. **33**, 045011 (2020).

[52] Y. L. Huang, Z. Feng, S. Ni, J. Li, W. Hu, S. Liu, Y. Mao, H. Zhou, F. Zhou, K. Jin, H. Wang, J. Yuan, X. Dong, and Z. Zhao, Superconducting (Li,Fe)OHFeSe film of high quality and high critical parameters, Chin. Phys. Lett. **34**, 077404 (2017).

[53] Y. Nakajima, Y. Tsuchiya, T. Taen, T. Tamegai, S. Okayasu, and M. Sasase, Enhancement of critical current density in Co-doped $BaFe_2As_2$ with columnar defects introduced by heavy-ion irradiation, Phys. Rev. B **80**, 012510 (2009).

[54] R. Prozorov, M. A. Tanatar, B. Roy, N. Ni, S. L. Bud'ko, P. C. Canfield, J. Hua, U. Welp, and W. K. Kwok, Magneto-optical study of $Ba(Fe_{1-x}M_x)_2As_2$ (M = Co and Ni) single crystals irradiated with heavy ions, Phys. Rev. B **81**, 094509 (2010).

[55] K. Itaka, T. Shibauchi, M. Yasugaki, T. Tamegai, and S. Okayasu, Asymmetric field profile in Bose glass phase of irradiated Y $Ba_2Cu_3O_{7-\delta}$: Loss of interlayer coherence around 1/3 of matching field, Phys. Rev. Lett. **86**, 5144 (2001).

[56] W. J. Li, S. Pyon, A. Yagi, C. Yu, R. Sakagami, A. Ichinose, S. Okayasu, and T. Tamegai, Peak effects induced by particle irradiations in $2H$-$NbSe_2$, Supercond. Sci. Technol. **36**, 115018 (2023).

[57] L. Civale, A. D. Marwick, T. K. Worthington, M. A. Kirk, J. R. Thompson, L. Krusin-Elbaum, Y. Sun, J. R. Clem, and F. Holtzberg, Vortex confinement by columnar defects in $YBa_2Cu_3O_7$ crystals: Enhanced pinning at high fields and temperatures, Phys. Rev. Lett. **67**, 648 (1991).

[58] G. Blatter, M. V. Feigel'man, V. B. Geshkenbein, A. I. Larkin, and V. M. Vinokur, Vortices in high-temperature superconductors, Rev. Mod. Phys. **66**, 1125 (1994).

[59] K. Tsuchiya, X. Wang, S. Fujita, A. Ichinose, K. Yamada, A. Terashima, and A. Kikuchi, Superconducting properties of commercial REBCO-coated conductors with artificial pinning centers, Supercond. Sci. Technol. **34**, 105005 (2021).

[60] C. J. van der Beek, M. Konczykowski, T. W. Li, P. H. Kes, and W. Benoit, Large effect of columnar defects on the thermodynamic properties of $Bi_2Sr_2CaCu_2O_8$ single crystals, Phys. Rev. B **54**, R792 (1996).

[61] T. Tamegai, W. Li, J. Wang, Y. Zu, A. Takahashi, S. Pyon, S. Okayasu, and A. Ichinose, Anomalous peak effects in superconductors with columnar defects, JPS Conf. Proc. **38**, 011026 (2023).

[62] W. Li, S. Pyon, S. Okayasu, and T. Tamegai, Peak effects in $2H$-$NbSe_2$ single crystals induced by particle irradiations, J. Phys.: Conf. Ser. **1975**, 012003 (2021).

[63] S. Eley, K. Khilstrom, R. Fotovat, Z. L. Xiao, A. Chen, D. Chen, M. Leroux, U. Welp, W. Kwok, and L. Civale, Glassy dynamics in a heavy ion irradiated $NbSe_2$ crystal, Sci. Rep. **8**, 13162 (2018).

[64] A. Takahashi, S. Pyon, T. Kambara, A. Yoshida, and T. Tamegai, Effects of asymmetric splayed columnar defects on the anomalous peak effect in $Ba_{0.6}K_{0.4}Fe_2As_2$, J. Phys. Soc. Jpn. **89**, 094705 (2020).

[65] T. Hwa, P. L. Doussal, D. R. Nelson, and V. M. Vinokur, Flux pinning and forced vortex entanglement by splayed columnar defects, Phys. Rev. Lett. **71**, 3545 (1993).

[66] T. Shibauchi, T. Nakano, M. Sato, T. Kisu, N. Kameda, N. Okuda, S. Ooi, and T. Tamegai, Interlayer phase coherence in the vortex matter phases of $Bi_2Sr_2Ca\ Cu_2O_{8+y}$, Phys. Rev. Lett. **83**, 1010 (1999).